Acoustic Noise Mitigation of Switched Reluctance Machines with Windows in Both Stator and Rotor Poles

Mohammed Elamin[1] Yusuf Yasa[1] Omer Gundogmus[1] Yilmaz Sozer[1]
John Kutz[2] Joshua Tylenda[3] Ronnie L. Wright[2]

[1]ECE Department,
University of Akron,
Akron, OH

[2]DCS Corporation,
Alexandria, VA

[3]US ARMY TARDEC,
Warren, MI

Abstract—**Switched Reluctance Machines (SRMs) have been studied by many researchers as an alternative to other types of electrical machines for use in electric and hybrid vehicle applications. SRMs are fault tolerant and have wide speed operating range. However, they suffer from several disadvantages including high vibration, acoustic noise and torque ripple. In this paper, placement of rectangular windows in both the rotor and stator poles is proposed to reduce the vibration and acoustic noise of SRMs. The position and the dimensions of the windows are optimized through Electromagnetic Finite Element Analysis (FEA). Multi-physics FEA is also performed to predict the vibration and acoustic noise of the optimized design. The results of this study confirm that placing windows in both the stator and the rotor of the SRMs can significantly reduce the acoustic noise compared to conventional SRMs.**

Keywords— Switch Reluctance Machine, Acoustic Noise, Vibration, Noise Reduction

I. INTRODUCTION

SRMs have many advantages over other electric machine types, such as: robustness, simple construction, low cost, high torque/inertia ratio, wide speed range, better thermal performance, fault tolerance, and reliability [1]. These attractions make SRMs a strong candidate in many applications, such as space and aviation, or other harsh environment applications. However, the development of SRM for use in the automotive industry and home appliances has been limited mostly due to the high torque ripple and high acoustic noise and vibration [2].

For the last two decades many studies have been conducted to mitigate the noise and vibration of SRMs. These studies can be classified into two main categories: control approaches or geometrical design modifications.

Regarding the control approach of current shaping, one of the main methods is active vibration cancellation (AVC) [3]. In this method, during the demagnetization stage, a period of zero voltage is applied to the winding to cancel the free vibration. In [4] a hybrid excitation method has been proposed. Where, two phases are excited by a long conduction angle and one phase by conventional angles to smooth the abrupt change of the excitation. In [5] direct instantaneous force control was used to smooth the force sum by shaping the current and eliminate mode-0 borne noise. A special current waveform has been proposed in [6] to reduce the acoustic noise and vibration excited by the third harmonic of the radial force sum. Control techniques increase the computational complexity, have a negative impact on the drive performance, but are not effective over the entire speed range.

With respect to the geometrical design approach; many unconventional SRM design concepts have been proposed to improve the machine characteristic, such as having double stator structure or shark type SRMs [7]-[9], while other researchers follow the path to improve the design of the conventional SRM. In [10], the effects of different machine frame shapes were studied. In [11], authors propose to use structural spacers between the poles. The authors in [12] indicated that having a higher number of rotor and stator poles is always better from the noise perspective. Different stator pole shape and yoke designs have been investigated in [13], [14]. Skewing the stator and/or rotor laminations are studied in [15].

Making windows in SRM structure is also one of the methods reported in the literature. In [16], [17] three different rectangular windows are introduced in the rotor and the static radial force and torque was calculated for each configuration to determine the best method. Also, the effect of different circular windows in the rotor poles and yoke is studied in [18], [19] respectively. In [20], the authors focused on creating windows in only rotor or stator lamination. Comparison of these methods shows that individually windowed stator or rotor SRM has a similar effect; as both methods have successfully reduce the peak value of acoustic noise compared with the non-windowed SRM.

In this study rectangular windows in both the stator and rotor poles are applied to a case study SRM. The coupled circuit and the FEA simulations are conducted at the rated conditions. An optimization method to determine the best dimensions and position of the windows is carried out. Mechanical FEA

analysis is performed to predict the deformation and acoustic noise of SRM with the optimized windows. The electromagnetic, mechanical, and acoustic performance of the windowed SRM are compared with the conventional SRM at the same operating conditions.

II. NOISE GENERATION IN SRM

The acoustic noise in SRMs can arise from electromagnetic, mechanical, or aerodynamic causes. The mechanical noise may emanate from the gearbox, bearing friction, mechanical misalignment or eccentricity. Aerodynamic noise can be caused by ventilation fans or air flowing through rotor salient poles, especially at high speeds. Electromagnetic noise is caused due to the magnetic flux in the air gap. The electromagnetic noise contributes the majority of acoustic noise in SRMs [21].

The magnetic flux in electrical machines passing through the air gap can be decomposed into radial and tangential component. The magnetic flux densities generate radial and tangential forces on stator and rotor poles as shown in Fig. 1. The tangential component acts on the rotor teeth surfaces generating the torque and tangential vibration on the stator teeth. The tangential vibration is very small and the majority of vibration and acoustic noise are caused by the force acting on the stator pole tips at the radial direction [22]. In SRMs, the variation of the radial force is very large compared to smooth airgap machines due to the saliency structure and the phase commutation.

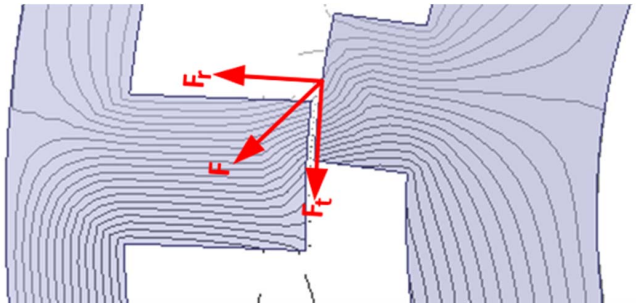

Fig. 1. Magnetic flux lines nad forces in the air gap

There are several methods to calculate the magnetic forces in the air gap such as: global virtual work method, the Maxwell stress- tensor method, the Coulomb virtual work method and the Lorentz force formula [23]. Among these methods Maxwell stres tensor can be used to calculate the force on the air gap. The stress tensor T can be expressed as in (1), where B is flux density, μ_0 is the permeability of free space and $\hat{n}$ is the unit normal vector. The force F acting on the integral surface (s) can be presented by (2) and correspondingly, the tangential force, F_t, and radial forces, F_r, can be expressed as in (3) and (4), respectively. In these formulations, B_r and B_t are the radial and tangential component of the flux density in the air gap respectively.

$$T = \frac{1}{\mu_0}\left[(\vec{B}\cdot\hat{n})\vec{B} - \frac{1}{2}\nabla B^2\hat{n}\right] \quad (1)$$

$$F = \int T\, ds \quad (2)$$

$$F_t = \iint \frac{1}{\mu_0}(\vec{B}\cdot\hat{n})\vec{B}\, ds = \frac{1}{\mu_0}\iint \vec{B}_r\vec{B}_t\, ds \quad (3)$$

$$F_r = \iint \frac{1}{2\mu_0}\nabla B^2\hat{n} = \frac{1}{2\mu_0}\iint ({B_r}^2 - {B_t}^2)\, ds \quad (4)$$

Natural frequencies of the machine structure are very critical in generating the vibration and the acoustic noise. When one of the radial force harmonics coincide with one of the natural frequencies of stator/frame structure, resonance will occur. The resonance will cause SRM structure to deform and vibrate with the specific mode shapes. The vibration of the outer surface creates a pressure in the surrounding air generating airborne acoustic noise. The vibration caused by the radial force will often form along the circumference of the stator surface. The first six circumferential mode shapes of the cylindrical machines are shown in Fig. 2. For small machines modes 1-4 are more significant; however, for large and medium machines higher vibration modes are more pronounced [24]. Mode 2 (oval shape) of the structure is the dominant mode in SRMs having two poles per phase [25], while mode 4 (double oval shape) is more common on SRMs having four poles per phase [12]. For SRMs having a high number of poles, mode 0 (the pulsating or breathing mode) is the most common [5]. The pulsating mode causes uniform deformation along the outer surface of the stator.

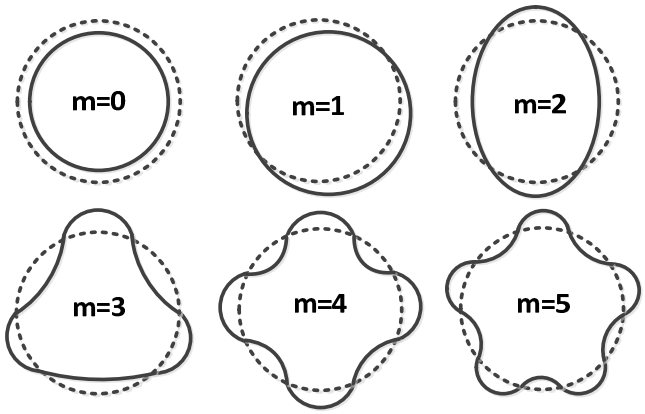

Fig. 2. Circumferential mode shapes of cylindrical machines.

III. SRM WITH WINDOWS IN STATOR AND ROTOR POLES FOR NOISE REDUCTION

The radial forces are reported to be the main source of noise and vibration in SRMs. The magnitude of the radial force depends on the magnetic flux density in the air gap as presented

in (4). One way to reduce the radial force in SRMs is to introduce windows in both the rotor and stator poles, which increases the reluctance of the magnetic circuit around the poles. This method reduces the radial force, but the tangential force and the torque production could be affected. For this reason, there is a need for an optimization process to determine the best place and dimensions of the windows in order to achieve the reduction in the radial force with minimum impact on the electromagnetic torque.

The parameters that define the windows in stator and rotor poles are shown in Fig. 3. Where D is the distance from the midpoints of the tooth tips, H is the height of the window and W is the width of the window. The effect of the windows on the reluctance of the magnetic circuit will depend on the variables D, W and H.

The performance of a noise reduction method can be evaluated through the measure of the peak radial force [17]-[19]. A different perspective, which is more suitable for SRMs with high number of poles, is the peak to peak variation of the total sum of the radial forces. In this method, the radial forces of adjacent poles is considered to be acting in small area of the stator yoke [5], [6]. The later method is considered in this research for the optimization and verification of the proposed noise reduction method.

A performance index (I) can be defined as in (5) to assess the effectiveness of each design, where T_{avg} the average torque is and F_{ripple} is the peak to peak value of radial force sum.

$$Performance\ Index\ (I) = \frac{T_{avg}}{F_{ripple}} \qquad (5)$$

The optimum design can be determined by sweeping the parameters in Fig. 3 in specific range and then select the one that maximizes the performance index (I).

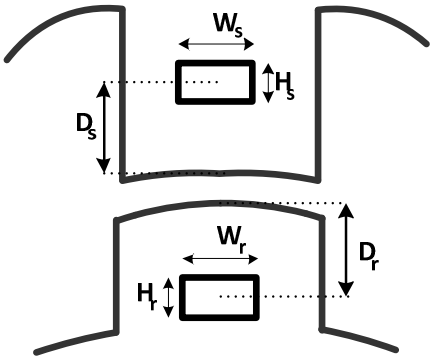

Fig. 3. Windows variables in both stator and rotor.

IV. SIMULATION AND ANALYSIS RESULTS

The study is performed in 24/16 three phase SRM. Firstly, the conventional (non-windowed) SRM is simulated through FEA at the rated condition to have a baseline. Then, the parameters provided in Fig. 3 are swept to get optimum window design for the stator and the rotor. Finally, multi-physics FEA is performed to predict and compare the vibration and noise levels of the baseline and the optimum windowed SRMs.

A. ELECTROMAGNETIC ANALYSIS

The average torque and force sum ripple are used to calculate the performance index of each design. The baseline SRM has a performance index of 0.6. There are 1070 different windows variations covered during optimization process. Figure 4 presents the optimization results, where each point indicates the percentage torque reduction versus the percentage of radial force ripple reduction compared to the baseline SRMs.

Below the 20 % torque reduction point, the force reduction increases linearly with the torque reduction. In this linear region, the points that are more close to the dashed red line of Fig. 4 are the best in reducing the force ripple for a given torque reduction. Beyond the linear region, there is no significant improvement in the force ripple reduction. The optimum design is determined based on the point having a maximum performance index (I) as shown in Fig. 4. The optimum design as shown in Fig. 5 has a 1.36 performance index with having 64.2 % force ripple reduction and 19.8% torque reduction.

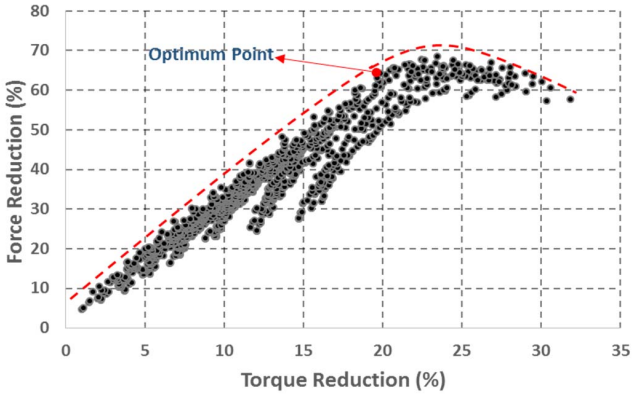

Fig. 4. Parametric sweep results of the windows.

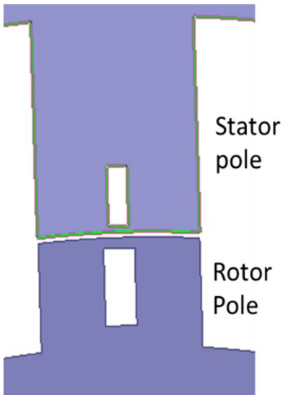

Fig. 5. Optimum stator and rotor windows

The normalized static torque production of the baseline and the proposed windowed SRM is presented in Fig. 6. It is observed that the windowed SRM output torque is reduced especially during the overlapping region of the poles. The reduction in the windowed SRM can be compensated for by increasing the peak current if the motor cooling can tolerate the increment in the temperature. Increasing the peak current by 20% produces an average torque that is only 4% less than the baseline SRM, while the force ripple is still reduced by 61% compared to the baseline SRM. The radial force contributed by each phases, as well as the total force ripple, is shown in Fig. 7. The performance index after increasing the current is 1.29 compared to 0.6 for the baseline SRM.

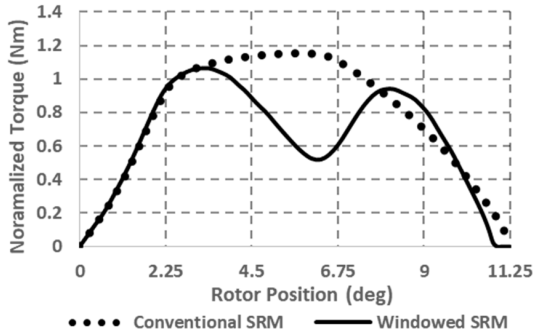

Fig. 6. Static torque characteristic

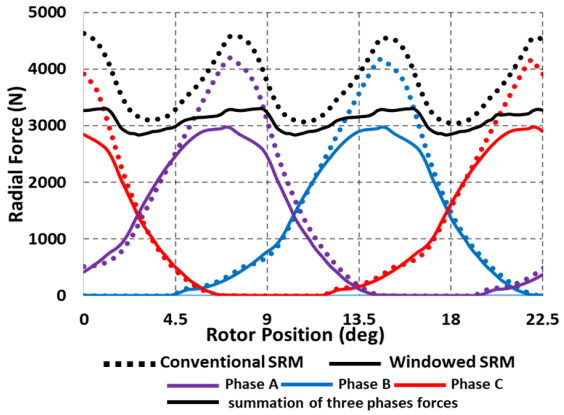

Fig. 7. The phase and the sum radial forces for the baseline and the windowed SRMs.

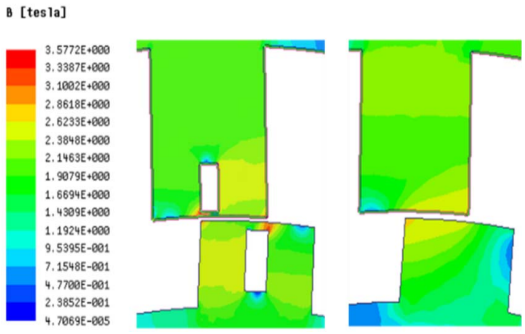

Fig. 8. Flux densities at the poles for the windowed and baseline SRMs.

Figure 8 presents the flux densities at the poles for the baseline and the optimum windowed SRMs. The windowed SRM has a slightly higher flux density compared to the conventional SRM. A flux saturation is present in small regions around the windows, which can be improved if a fillet is added around the corners of the windows.

B. VIBRATION AND ACOUSTIC ANALYSIS

Multi-physics FEA is performed to evaluate the effectiveness of the windowed SRM in reducing acoustic noise level compared to the baseline SRM. The flow diagram of multi-physics analysis is shown in Fig. 9. The frequency spectrum of the radial force, calculated through the electromagnetic FEA, is considered as an input to the mechanical FEA. The deformation, acceleration, and velocity is calculated in the frequency domain through the harmonic response and modal analysis. Finally, the velocity of the outer surface is transferred to the acoustic analysis to determine the sound pressure level (SPL) around the motor.

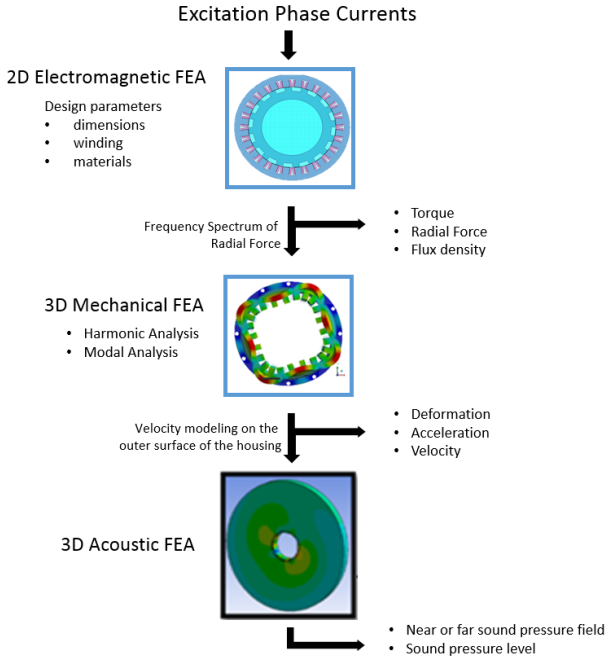

Fig. 9. The flow diagram of the multi-physics simulation.

The motor model used for the mechanical FEA analysis is presented in Fig. 10. In this model not only the stator structure but also the complete housing is modeled. The force spectrum on different stator poles is uploaded to the corresponding tooth tip in the mechanical model. The points where the motor assembly fixed to the test stand is considered as a fixed support in the analysis.

The acoustic FEA model is basically a body around the outer peripheral of the motor in the radial direction as shown in Fig. 11. The body has same properties as air regarding to the sound propagation. Radiation boundary conditions are assigned to the outer surface of the acoustic body. The mode shapes and their natural frequencies are calculated by using modal analysis. The mode shapes with m=0, 2 and 4 and their natural frequencies are

presented in Fig. 12. The peaks of the vibration and acoustic noise are expected to happen near these frequencies.

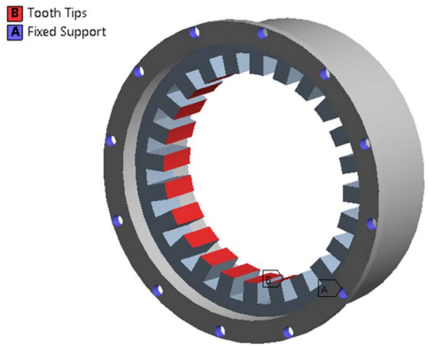

Fig. 10. FEA model of the SRM for mechanical FEA.

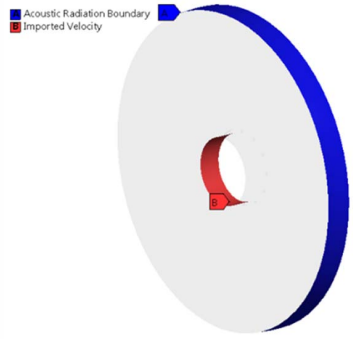

Fig. 11. FEA model of SRM for acoustic analysis.

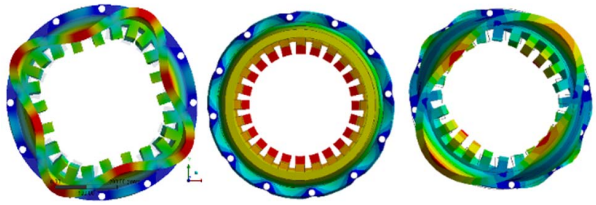

m4:1.96 kHz **m0: 2.44 kHz** **m2: 3.97 kHz**

Fig. 12. Dominant mode shapes of the baseline SRM.

The maximum deformation of the housing outer surface is shown in Fig. 13. The maximum deformation of the housing is reduced from 0.49 um for the baseline SRM to 0.24 um for the windowed SRM as shown in Fig. 13. The sound pressure level (SPL) at 1m distance from the outer surface of the motor is shown in Fig. 14. The peaks of the SPL are near the natural frequencies of the mode shapes with the maximum value happening near the frequency of the pulsating mode (m=0), which is expected for an SRM with a high pole count. The maximum simulated SPL level is reduced from 89.75 dB for the baseline SRM to 76.9 dB for the optimum windowed SRM.

Table II summarize the electromagnetic and mechanical performances of the baseline and windowed SRMs. The results present a considerable improvement on the performance index, maximum deformation and maximum noise level for the windowed SRM compared to baseline SRM. The tradeoff for using the windowing methods is a lower motor efficiency since higher current is needed to reach the same torque level. The lower efficiency operation can be observed by comparing the torque per ampere values for the baseline and the windowed SRM in Table II.

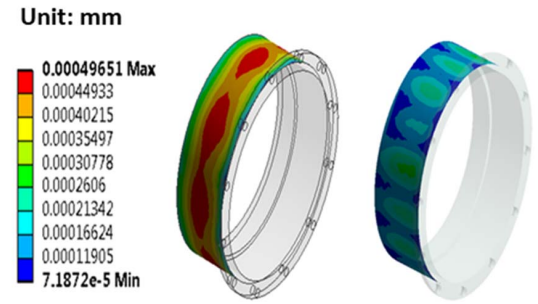

Fig. 13. deformation of the frame surface, (a) baseline SRM, (b) Windowed SRM.

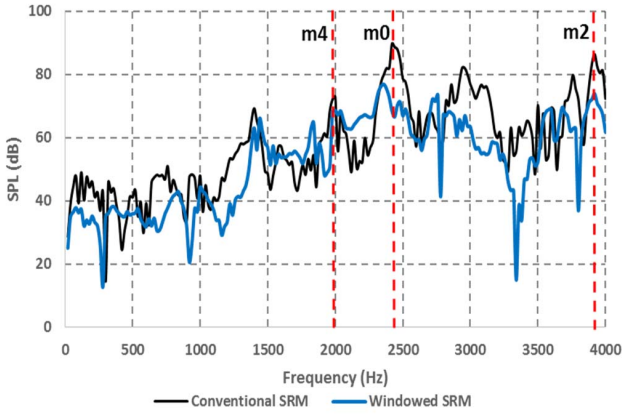

Fig. 14. Sound pressure level at one meter from the outer surface.

Table. 2. comparison of windowed SRM and Conventional SRM Performance

	Conventional SRM	Windowed SRM
Normalized Torque (Nm)	1	0.96
Torque per Ampere (Nm/A)	5.98	4.99
Performance Index (I)	0.6	1.29
Maximum Deformation (um)	0.49	0.24
Maximum SPL (dB)	89.75	76.9

V. CONCLUSION

In this paper, the effectiveness of placing windows in both stator and rotor poles has been investigated to reduce the vibration and noise levels of SRMs. An optimization process has been implemented to determine the best position and dimensions of the windows. A comparison between the optimized windowed SRM and the baseline SRM was conducted through multi-physics simulations. Results of the analysis shows that the peak sound pressure level and the corresponding acoustic noise are reduced significantly for the windowed SRM. This study proves that the windowed SRM is very effective in reducing the noise and vibration level of SRMs. The drawbacks of the windowed SRM include increasing the phase current to compensate for torque reduction and the higher flux density at the rotor and stator poles, which means more copper and iron loses and hence lower motor efficiency.

ACKNOWLEDGMENT

This paper draws on research funded by US Army Tank Automotive Development and Engineering Center (TARDEC).

REFERENCES

[1] B. Fahimi, A. Emadi, and R. B. Sepe, Jr., "A switched reluctance machine-based starter/alternator for more electric cars," *IEEE Trans. Energy Convers*. vol. 19, no. 1, pp. 116–124, Mar. 2004.

[2] M. Krishnamurthy, C.S. Edrington, A. Emadi, P. Asadi, M. Ehsani, B. Fahimi, "Making the case for applications of switched reluctance motor technology in automotive products," *IEEE Transactions on Power Electronics*, vol. 21, pp. 659-675, 2006.

[3] Z. Q. Zhu, X. Liu, and Z. Pan, "Analytical Model for Predicting Maximum Reduction Levels of Acoustic noise and vibration in Switched Reluctance Machine by Active Vibration Cancellation," *IEEE Trans. on Energy Convers.*, vol.26, no.1, pp.36-45, March 2011.

[4] J. W. Ahn, S. J. Park, and D. H. Lee, "Hybrid excitation of SRM for reduction of vibration and acoustic noise," *IEEE Trans. Ind. Electron.*, vol. 51, no. 2, pp. 374–380, Apr. 2004.

[5] A. Klein-Hessling, A. Hofmann and R. W. De Doncker, "Direct instantaneous torque and force control: a control approach for switched reluctance machines," *IET Electric Power Applications*, vol. 11, no. 5, pp. 935-943, 5 2017.

[6] M. Takiguchi, H. Sugimoto, N. Kurihara, A. Chiba, "Acoustic Noise and Vibration Reduction of SRM by Elimination of Third Harmonic Component in Sum of Radial Forces," *IEEE Trans. on Energy Convers.*, vol. 30, pp. 883 – 891, Sep. 2015.

[7] M. Abbasian, M. Moallem, and B. Fahimi, "Double-stator switched reluctance machines (dssrm): Fundamentals and magnetic force analysis," *IEEE Trans. Energy Convers.,* vol. 25, no. 3, pp. 589–597, Sep. 2010.

[8] A. Labak, and N. C. Kar, "Designing and Prototyping a Novel Five-Phase Pancake-Shaped Axial-Flux SRM for Electric Vehicle Application Through Dynamic FEA Incorporating Flux-Tube Modeling," *IEEE Trans. Ind. Appl.,* vol.49, no.3, pp.1276-1288, May-June 2013.

[9] P. O. Rasmussen, F. Blaabjerg, J. K. Pedersen, and F. Jensen, "Switched reluctance-shark machines more torque and less acoustic noise," *in Conf. Rec. IEEE- IAS Annu. Meeting*, vol. 1, 2000, pp. 93 – 98

[10] S. M. Castano, B. Bilgin, E. Fairall, and A. Emadi, "Acoustic noise analysiof a high-speed high-power switched reluctance machine: Frame effects," *IEEE Trans. on Energy Convers.*, vol. 31, no. 1, pp. 69–77, Mar. 2016.

[11] P. O. Rasmussen, J. H. Andreasen and J. M. Pijanowski, "Structural stator spacers-a solution for noise reduction of switched reluctance motors," *IEEE Trans. Ind. Appl.*, vol. 40, no. 2, pp. 574-581, Mar./Apr. 2004.

[12] J. Li, X. Song, and Y. Cho, "Comparison of 12/8 and 6/4 switched reluctance motor: noise and vibration aspects," *IEEE Trans. Magn.,* vol. 44, no. 11, pp. 4131–4134, Nov. 2008.

[13] J. P. Hong, K. H. Ha, and J. Lee, "Stator Pole and Yoke Design for Vibration Reduction of Switched Reluctance Motor," *IEEE Trans. on Magn.* vol. 38, no. 2, pp. 929 - 932, Mar. 2002.

[14] T. Kotegawa and I. Miki, "Stator structure for reducing noise in switched reluctance motor, " *2013 15th European Conference on Power Electronics and Applications (EPE)*, Lille, 2013, pp. 1-9.

[15] C. Gan, J. Wu, M. Shen, S. Yang, Y. Hu, and W. Cao, "Investigation of skewing effects on the vibration reduction of three-phase switched reluctance motors," *IEEE Trans. Magn.*, vol. 51, no. 9, pp. 1–9, 2015.

[16] M. Sanada, S. Morimoto, Y. Takeda, and N. Matsui, "Novel rotor pole design of switched reluctance motors to reduce the acoustic noise," *Industry Applications Conference, 2000. Conference Record of the 2000 IEEE* vol. 1, pp. 107-113, 2000.

[17] K. Nakata, K. Hiramoto, M. Sanada, S. Morimoto, and Y. Takeda, "Noise reduction for switched reluctance motor with a hole," in proc. *the Power Conversion Conference, 2002. PCC-Osaka 2002*, vol. 3, pp. 971-976, 2002.

[18] J. Li, H. X. Sun, and Y. Liu, "New rotor structure mitigating vibration and noise in switched reluctance motor," *2010 International Conference on Information, Networking and Automation (ICINA)*. vol. 2, pp. 80-84, 2010.

[19] J. Faiz, F. Tahvilipour, and G. Shahgholian, "Performance Improvement of a Switched Reluctance Motor," *PIERS Proc.*, pp. 728–732, 2012.

[20] M. Elamin, Y. Yasa, Y. Sozer, J. Kutz, J. Tylenda and R. L. Wright, "Effects of windows in stator and rotor poles of switched reluctance motors in reducing noise and vibration," *2017 IEEE International Electric Machines and Drives Conference (IEMDC)*, Miami, FL, 2017, pp. 1-6.

[21] M. N. Anwar, and I. Husain, "Radial force calculation and acoustic noise prediction in switched reluctance machines," *IEEE Trans. Ind. Appl.*, vol. 36, no. 6, pp. 1589–1597, 2000.

[22] C. Y. Wu and C. Pollock, "Analysis and reduction of vibration and acoustic noise in the switched reluctance drive," *IEEE Trans. Ind. Appl.*, vol. 31, no. 1, pp. 91–98, Jan./Feb. 1995.

[23] M. Moallem and C. M. Ong, "Predicting the torque of a switched reluctance machine from its finite element field solution," in *IEEE Transactions on Energy Conversion*, vol. 5, no. 4, pp. 733-739, Dec 1990.

[24] S. J. Yang, *Low-Noise Electrical Motors*. Oxford, U.K.: Clarendon.

[25] D. E. Cameron, J. H. Lang, and S. D. Umans, "The Origin and Reduction of Acoustic Noise in Doubly Salient Variable-Reluctance Motors," *IEEE Trans. Ind. Appl.*, vol. 28, no. 6, pp. 1250–1255, 1992.